ELSEVIER

Journal of Photochemistry and Photobiology A: Chemistry 126 (1999) 1–5

Journal of Photochemistry and Photobiology A:Chemistry

www.elsevier.nl/locate/jphotochem

The influence of solute absorbance in laser flash photolysis – actinometry in experiment and theory at non-vanishing absorbance

Justus von Sonntag *

Institut für Oberflächenmodifizierung, IOM e.V., Permoserstraße 15, D-04303 Leipzig, Germany

Accepted 6 May 1999

Abstract

Laser flash photolysis set-ups are commonly operated with non-vanishing absorbance in order to obtain a maximum signal-to-noise ratio. The exponential law of light absorption leads to non-linear equations. An example of their mathematical treatment is given and compared with experiments using the benzophenone-4-carboxylic acid actinometer (excitation wavelength: 308 nm) up to a solute absorbance of 6. The influence of geometry in concert with solute absorbance on the signal reading is modelled. Two approximated mathematical solutions of the ensuing non-linear equations are presented together with their application for an optimisation of laser flash photolysis experiments.

Keywords: Actinometry; Laser flash photolysis; Benzophenone-4-carboxylic acid; Mathematical model

1. Introduction

In photochemistry, laser flash photolysis is the tool of choice for the investigation of fast reactions. A typical set-up comprises an optical detection system capable of following the build-up and decay of transient absorption on the ns- to ms-timescale and a pulsed laser with short (<100 ns) pulses of high energy (>5 mJ) to generate the excited species. The method is usually applied to measure the rate of reactions, but is also (and commonly) used to provide quantitative data on yields and transient absorption spectra.

To achieve this goal, the total amount of 'active' absorbed photons has to be determined. Laser energy output is commonly monitored by a calorimeter. While calorimetry gives a direct physical reading of the energy dissipated onto a surface, it cannot take into account the processes occurring in the cuvette itself. Chemical actinometry, on the other hand, does precisely that; it uses the same measuring devices as the sample and therefore shows the same behaviour. All effects occurring outside the cuvette walls are the same for actinometry and the laser flash photolysis experiment; and hence are intrinsically compensated for.

2. Rationale for using high solute absorbance

There are several reasons to use high to very high solute absorbance. In laser flash photolysis the total noise is governed by the noise from the photomultiplier and the lamp photon current and therefore almost independent of signal strength. The signal-to-noise ratio is thus improved by increasing the signal strength. The signal strength is a function of solute absorbance as will be shown in Fig. 2. In certain cases, the concentration of the ground state molecule may be of importance, e.g. in competition kinetics [1]. In those cases the concentrations to be used are then governed by the ratio of rate constants; the absorbance can, of course, not be set independently. A third aim is the suppression of biphotonic reactions, as the low concentration of excited molecules cannot compete effectively for photons if the absorbance by ground state molecules is very high.

3. Experimental

Benzophenone-4-carboxylic acid (Lancaster) was used as received and dissolved in alkaline (sodium hydroxide) Milli-Q-filtered (Millipore) water.

The laser photolysis set-up comprises a 308 nm XeCl-excimer laser (MINex, LTB Berlin, pulse train of three pulses (70, 20 and 10% of total energy, respectively), each with 5 ns half width, all three within 70 ns, total pulse train energy up

* Fax: +49-341-235-2584
E-mail address: justus@rz.uni-leipzig.de (J. von Sonntag)

1010-6030/99/$ – see front matter
PII: S1010-6030(99)00104-5

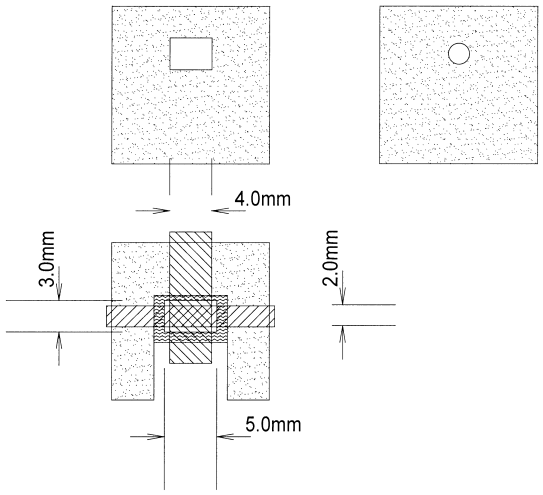

Fig. 1. The geometry of the cuvette screen. Dotted areas: screen, made of aluminium; zigzagged area: cuvette. Hatched areas: light paths, laser: from top to bottom, analysing-light: from left to right. Doubly hatched: overlapped volume of exciting (laser) and analysing-light, forming a cylinder.

to 15 mJ) as excitation source and a pulsed xenon short-arc lamp (XBO 450, Osram, power supply LPS 1200, Photon Technology International) supplying the analysing-light. The lamp pulser (MCP 2010, Photon Technology International) is operated at 178 A and 3.3 ms pulse duration. A motorised circular neutral density filter is used to keep the light intensity reaching the photomultiplier (1P28, Hamamatsu, operated at 900 V, power supply: PS310, Stanford Research Systems) through the monochromator (Triax 190, ISA Jobin Yvon-Spex) within its linearity range. A 500 MHz, 2.5 GS/s digitising storage oscilloscope (TDS620b, Tektronix) operates as transient recorder. A small fraction of the laser beam is coupled out with a thin quartz plate and directed onto a photodiode (SB 103, RFT). Its reading is fed into a second oscilloscope (TDS 520, Tektronix) as a measure for the pulse energy. The area under the signal was compared with a bolometer reading and found to be linear with laser pulse energy. This area is used to normalise the measured spectra to constant energy to correct for the long term variations of the energy delivered as well as the fluctuations between pulses. The photodiode signal is also used for triggering the transient recorder.

The pathlength of the flow-through suprasil quartz cell is 5 mm in the analysing-light and 3 mm in the laser light direction. The sample duct is made entirely from glass, with the flow being set to ensure a complete exchange of sample between laser pulses by creating a small pressure difference between waste and feed beaker. In order to be able to start and stop the flow this pressure difference is provided by a small pump. This pump does not come into contact with the sample but creates the pressure difference by pumping off the air above the waste solution which is being refed into the waste beaker through a ballast valve. The feed can be purged with nitrogen, but for this actinometer system it was not necessary.

The complete set-up is computer controlled by a custom-made program. A timing I/O board (PC-TIO-10, National Instruments) is used as trigger delay generator. The laser, lamp pulser, lamp and laser shutters (both custom-made) are triggered with opto-decoupled TTL-pulses. The laser shutter is kept closed while measuring the baseline, the lamp shutter only opens for some ms before the laser pulse to avoid unnecessary exposure of the sample to the high-intensity analysing-light.

A 16-fold accumulation was used to improve signal-to-noise ratio, the baseline was accumulated 4 times and fitted by a polynomial to remove high-frequency noise.

A screen for the cuvette, shown in Fig. 1, was made. This cuts from the analysing-light a circle of 2 mm diameter which is overlapped by a 4 mm × 3 mm square cut from the laser beam.

4. Results and discussion

The main problem of using a laser flash photolysis set-up for quantitative spectra is the setting of a correct geometry for both excitation and analysing-light. The laser emits a coherent, parallel beam of approximately uniform distribution. The analysing-light, incident at normal angle to the laser beam, is emitted over a certain volume by a, usually pulsed, xenon short-arc lamp. Its projection area is typically an oval with a size of 2 mm × 3 mm. The light is then collimated, (filtered etc.) and refocused into the cuvette. The output from the lamp is unfortunately not uniform. A compromise has to be made between using maximum light intensity and a reasonably uniform light distribution. The screen mentioned above served this purpose by using the entire focal area of the xenon short-arc but cutting the halo out. Similar screens are in widespread use, and the following calculations can easily be adapted to the reader's set-up.

If the source were a mathematical point the collimated light would be perfectly parallel and the light path would take the shape of a double cone, a diabolo. This would be unfortunate, as the focus would have to be set extremely accurately, and the light intensity in the focus would become very high. Collimated and refocused light from an extended source on the other hand does not produce a double cone with a focal point in the middle but shows a waist whose size depends on the width of the focal area of the lamp multiplied by the ratio of the focal lengths of the collimating and focussing lenses. Since the aperture of the screen has the same size, the light path has the shape of a cylinder. The laser beam is set in a way to completely overlap this cylinder. The aperture for the laser beam sets the pathlength of the cylinder in the analysing-light direction (in our case 4 mm). This cylinder is illustrated by the doubly hatched area in Fig. 1.

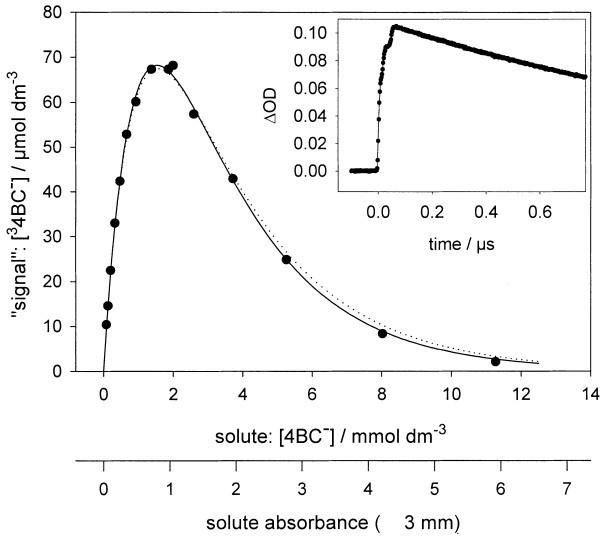

Fig. 2. Plot of the signal (benzophenone-4-carboxylate triplet) concentration vs. actinometer concentration. Filled symbols: experimental values, solid line: Eq. (6b), dotted line Eq. (6a), both with $x_C = 1.75$ mm and $d = 2$ mm. The flux is fitted by a Levenburg–Marquardt algorithm to least squares and amounts to 2.0×10^{-8} Einstein, $\hat{=}7.7$ mJ [3]. In the inset a typical time profile of the transient absorbance at 340 nm ([benzophenone-4 carboxylate] = 0.325 mmol dm^{-3}).

4.1. The laser flash photolysis experiment

Solutions of benzophenone-4-carboxylate ($4BC^-$) were made up in alkaline water in the concentration range of 8.2×10^{-5} to 1.13×10^{-2} mol dm^{-3}, corresponding to an absorbance in laser direction (3 mm pathlength) of 0.043 to 5.9. The actinometry is based upon measuring the transient absorbance of the triplet of the benzophenone-4-carboxylate anion (^{3}4BC$^-$, ε (at 340 nm) = 8800 dm^3 mol^{-1} cm^{-1}, quantum yield $\Phi = 1$ [2]) right after the pulse (at 70 ns). The intersystem crossing occurs on the picosecond timescale and the ^{3}4BC$^-$ decays under aerobic conditions only within some μs, cf. inset in Fig. 2. To distinguish between the local ^{3}4BC$^-$ concentration and the measured, average 'active' ^{3}4BC$^-$ concentration, the latter will be called 'signal' concentration. The oscilloscope signal is converted into transient concentration by dividing the common logarithm of the oscilloscope trace divided by its baseline by the pathlength (4 mm) and the molar absorption coefficient of the transient. A plot of the signal concentration versus actinometer concentration is shown in Fig. 2. The data show a steep increase in signal with increasing actinometer concentration, leading to a maximum. After that, an inflection point is encountered as the signal concentration approaches zero at high actinometer concentration.

4.2. Modelling

The behaviour of the experimental data cannot be described by a polynomial. The minimal empirical description is the difference of two exponential functions, with a total of three parameters. Such formulae are very ill-conditioned for numerical fitting with the conventional Levenburg–Marquardt algorithms [3]. A large number of local minima is encountered.

Therefore, the photophysics of the geometry as described above has been modelled. This has been done by multiplying the number of absorbed photons per differential volume element with a function describing whether or not this volume element is inside the cylinder and by summing up over all relevant volume elements.

According to Lambert–Beer's law, the number of quanta absorbed is proportional to the incident light intensity (I_0), the concentration of absorbing species (c_a) times a constant (the decadic molar absorption coefficient, ε_a), and the pathlength through the medium (x) [4]. Upon integration the well-known Eq. (1) is obtained (for ease of handling the product of the constants –ln(10), ε_a and c_a, is referred to as E) [4].

$$I(x) = I_0(\exp(-\ln(10)\varepsilon_a c_a x)) =: I_0 \exp(Ex) \tag{1}$$

The build-up of space-resolved product concentration $\Delta c_s(x)$ is described by Eq. (2), with Φ being the quantum yield of generation of the transient absorbing species [4].

$$\Delta c_s(x) = -\Phi \frac{dI}{dx} \tag{2}$$

The 'signal' concentration $\Delta\bar{c}_s$ is composed of the integration of the signal concentration in a certain volume element over all relevant volume elements. As the laser light intensity is practically uniform in analysing-light direction, the problem can be reduced from describing a cylinder to describing a circle with an area A.

$$\Delta\bar{c}_s = \Phi \frac{1}{A} \int_A -\frac{dI(x)}{dx}\, dA(x)$$
$$= -\Phi\, I_0 E \frac{1}{A} \int_A \exp(Ex)\, dA(x) \tag{3}$$

The circle can finally be reduced to a one-dimensional problem by substituting it by the product of the height of the segment perpendicular to laser and analysing-light direction and the differential width to this element.

Introduction of the geometrical constants of the circle, diameter d and centre x_C leads to Eq. (4). To exclude the parts not covered by the analysing-light, the x-transformed integration limits x_S and x_E are set as the beginning and end of the circle.

$$dA(x) = \sqrt{\frac{1}{4}d^2 - (x - x_c)^2}\, dx \;\Big|\; x_S = x_C - \frac{1}{2}d,$$
$$x_E = x_C + \frac{1}{2}d, \quad x \in [x_E, x_S] \tag{4}$$

The resulting integral can hardly be solved analytically and therefore two approximations will be discussed in the following. The rectangular approximation will be referred

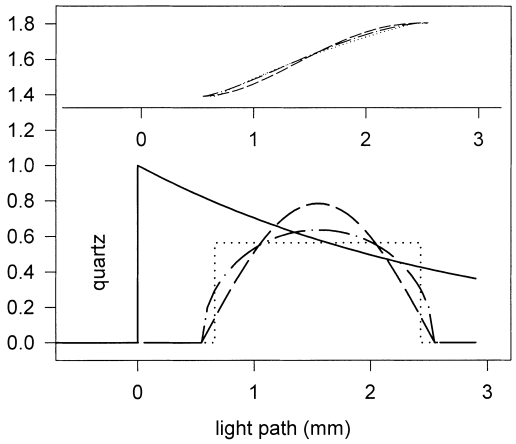

Fig. 3. Graphical description of the approximations relevant to the modelling. The light path is taken in laser beam direction and starts after the quartz cuvette wall; the aperture for the analysing beam starts at 0.55 mm and has a diameter of 2 mm. Solid line: relative product concentration (the laser light intensity follows naturally the same curve) at a $4BC^-$-concentration of 2 mmol dm^{-3}, dash-dot: circle, dashed line cosine approximation, dotted line: rectangular approximation. The three latter curves are normalised to an area of 1. In the upper part: cumulative area of Eq. (5a) (dotted) and (5b) (dashed) compared to the analogous function with a true circle. The endpoint of all three functions coincides within much less than 0.1%.

to with an 'a' behind the equation number, the cosine approximation with a 'b'. Most simply, the circle can be approximated by a square of the same area, with modified integration boundaries x'_S and x'_E Eq. (4a).

$$\mathrm{d}A(x) = \sqrt{\frac{\pi}{4}}d\,\mathrm{d}x \;\Big|\; x'_S = x_c - \frac{1}{2}\sqrt{\frac{\pi}{4}}d,$$
$$x'_E = x_C + \frac{1}{2}\sqrt{\frac{\pi}{4}}d, \quad x \in [x'_E, x'_S] \tag{4a}$$

The cosine function, Eq. (4b), approximates a circle better and the resulting integral, Eq. (5b), can still be solved analytically.

$$\mathrm{d}A(x) = \pi\cos\left(\pi\frac{x - x_C}{d}\right)d\,\mathrm{d}x \;\Big|\; x_S = x_C - \frac{1}{2}d,$$
$$x_E = x_C + \frac{1}{2}d, \quad x \in [x_E, x_S] \tag{4b}$$

The true centre x_C is determined by measuring the distance of the analysing-light aperture hole from the inner wall of the screen in laser direction and by subtracting the quartz thickness of the cuvette. A different method is the use of x_C as a fitting parameter in Eq. (6a) or (6b). The results agree within the accuracy of the vernier calliper (0.05 mm). The approximations (4a) and (4b) are depicted together with the true circle in Fig. 3.

Finally, all contributions are combined in one Equation (Eqs. (5a), (5b)).

$$\Delta\bar{c}_S = -I_0\Phi\frac{1}{d}\sqrt{\frac{4}{\pi}}E\int_{x=x'_S}^{x=x'_E}(\exp(Ex))\,\mathrm{d}x \tag{5a}$$

$$\Delta\bar{c}_S = -I_0\Phi\frac{\pi}{4d}E\int_{x=x_S}^{x=x_E}(\exp(Ex))\cos\left(\pi\frac{x - x_C}{d}\right)\mathrm{d}x \tag{5b}$$

The upper part of Fig. 3 shows the integrals of the product of triplet concentration and area (Eqs. (5a) and (5b)) together with a numerical integration of the true circle (Eq. (3)).

After expanding the cosine function with the appropriate addition theorem [5] and solving both resulting, tabellised [5] integrals, one can reorganise the result using the trigonometric addition theorems. The integration went from the beginning of the circle to its end, and therefore the trigonometric functions can be replaced by their values, leading to Eq. (6b). The integration of the rectangular approximation (5a) produces Eq. (6a).

$$\Delta\bar{c}_S = -I_0\Phi\frac{1}{d}\sqrt{\frac{4}{\pi}}(\exp(Ex'_E) - \exp(Ex'_S)) \tag{6a}$$

$$\Delta\bar{c}_S = -I_0\Phi\frac{\pi}{d^2}\frac{E}{E^2 + (\pi/d)^2}(\exp(Ex_E) + \exp(Ex_S)) \tag{6b}$$

The results of Eqs. (6a) and (6b) are both shown in Fig. 2, dotted and solid lines, respectively (with $x_c = 1.75$ mm and $d = 2$ mm). The (minute) shortcomings of the rectangular approximation are visible from Fig. 2: the shading due to the sample thickness before the analysing-light aperture is slightly underestimated at high concentrations. The use of the rectangular geometry is recommended, however, for slit apertures or a more complex geometry. An aperture with the shape of the focal area of the xenon short-arc, an oval of 2 mm × 3 mm, can, for example, be produced by a milling cutter in order to achieve a maximum analysing-light intensity (which is of particular interest in the short-wavelength region).

4.3. Product absorbance

Upon excitation products are formed that absorb light, too. This feature has consequences for the modelling of the photophysics occurring in the cuvette. The product absorbance in direction of the excitation (laser) light can be neglected as long as it is small in comparison with the solute absorbance. As the product concentration is proportional to the laser beam energy density (Eq. (2)), a simple attenuation of the laser beam can always be used to meet this criterion. If the total number of excited particles is to be kept, the pathlength of the cuvette in analysing-light can be increased and the laser beam appropriately focussed. By this method the energy density is decreased without decreasing the total energy delivered. The disadvantage is that the sample consumption increases with increasing illuminated volume and the solute absorbance increases in analysing-light direction as well. This means that there is less analysis-light left to reach the photomultiplier, leading to small and therefore noisy signals.

It is obvious, that the product does also absorb light in the analysing-light direction. The product concentration is, however, not uniform, as depicted by the solid line in Fig. 3. The photomultiplier does not give a space-resolved signal, it is proportional to the sum of all photons arriving at a given time. The 'signal absorbance' is determined by taking the common logarithm of the ratio of the photomultiplier reading and its base-line. In principle, one would have to use the true exponential description and actually sum up over the exponential of the argument of the integral in Eq. (3). This is depicted in Eq. (7), with $I_A(x)$ being the space-resolved analysing-light intensity with transient absorption, $I_{A,0}$ the baseline, ε_A the decadic molar absorption coefficient of the transient ($8800\,\mathrm{dm^3\,mol^{-1}\,cm^{-1}}$ at 340 nm) and x_A the analysing-light pathlength covered by the laser beam (4 mm).

$$I_{\mathrm{A}}(x) = I_{A,0}\exp(-\ln(10))\varepsilon_A x_A \Delta c_{\mathrm{S}}(x)) \Rightarrow \overline{I}_A = I_{A,0}\frac{1}{A}\int_0^A \exp\left[(\ln(10))\varepsilon_A x_A \Phi I_0 E \exp(Ex)\right] \mathrm{d}A \tag{7}$$

The exponential function can easily be developed into a Taylor's series. If this series is terminated after its first two terms, it is linear. For small value of the argument, the approximation is acceptable (the error is <10% for an absorbance <0.18). This maximum absorbance of the transient (in contrast to the solute absorbance) in this work does not exceed this limit and this holds even more true for the difference in absorbance from one side of the aperture to the other. Therefore, the simplification of using a linear relationship of absorbance and mean transient concentration (Eq. (8)) is justified.

$$\overline{I}_A \approx I_{A,0}\exp(-\ln(10)\varepsilon_A x_A \Delta\overline{c}_{\mathrm{S}}) \left| -\log\left(\frac{\overline{I}_A}{I_{A,0}}\right) \leq 0.18 \right. \tag{8}$$

5. Conclusion

Two (approximated) solutions for the equation describing the correlation between solute absorbance and measured product concentration have been presented. They are developed entirely from independently measurable quantities and do not rely on calibration values or curves. This results in a description of the shape of the signal versus solute absorbance-relationship with no adjustable parameters, in contrast to commonly applied formulae [6]. Only the amplitude of the curve (Fig. 2) results from fitting with just one adjustable parameter, the 'active' incident laser light density, as this quantity is difficult to access independently.

The Eqs. (6a) and (6b) are explicit in 'signal' concentration, $\Delta\overline{c}_{\mathrm{S}}$, and can trivially be made explicit in laser beam intensity, I_0. One of the applications of the formulae is the calculation of active product concentration if the absorbance of sample and actinometer solution used differ. This avoids the tedious adjusting of their absorbance commonly used, e.g. [7]. For that purpose one has to determine the incident laser light flux I_0 from the actinometer signal with the actinometer absorbance and then calculate the product of quantum yield and active product concentration $\Delta\overline{c}_{\mathrm{S}}$ with the sample absorbance.

The model presented here can also be used to optimise experimental conditions. The absorbance for maximum signal concentration can, for example, be calculated. For set-ups of similar geometries (ratio of analysing-light aperture diameter to total laser beam direction pathlength) this is, as a numerical analysis of Eq. (6a) shows, independent of the cuvette size. For a set-up with a reasonable part (50–90%) of the laser beam pathlength covered by the analysing-light the maximum 'signal' concentration will be achieved with an absorbance between 0.6–1.1.

Another topic worth mentioning is the determination of second-order rate constants. There, a uniform product concentration has to be assumed. This is, strictly speaking, never the case in laser flash photolysis. However, the model allows the calculation of the concentration distribution throughout the sample cell. This can be used to determine the deviation from true second-order kinetics encountered in the experiment.

Acknowledgements

The author wishes to acknowledge Dr. Knolle for useful discussions, Dr. Naumov for double-checking the mathematics and Professor Mehnert for continuous interest and support.

References

[1] J. von Sonntag, D. Beckert, W. Knolle, R. Mehnert, Radiat, Phys. Chem. 55 (1999) 609–613.
[2] J.K. Hurley, H. Linschitz, A.J. Treinin, J. Phys. Chem. 92 (1988) 5151–5159.
[3] AISN Software Inc., TableCurve2D Automated Curve Fitting Software User's Manual, Jandel Corporation, San Rafael, 1994
[4] R.V. Benssason, E.J. Land, T.G. Truscott, Excites States and Free Radicals in Biology and Medicine. Contributions from Flash Photolysis and Pulse Radiolysis, Oxford University Press, Oxford, 1993
[5] I.N. Bronstein, K.A. Semendjajew, Taschenbuch der Mathematik, Deutsch, Frankfurt am Main, 1979
[6] N.K. Shrestha, E.J. Yagi, Y. Takatori, A. Kawai, Y. Kajii, K. Shibuya, K. Obi, J. Photochem. Photobiol. A: Chem. 116 (1998) 179–185.
[7] B. Marciniak, E. Andrzejewska, G.L. Hug, J. Photochem. Photobiol. A: Chem. 112 (1998) 21–28.